DOI : *10.15613/sijrs/2023/v10i1-2/44111*
ISSN (Print): 2349-8919
ISSN (Online): 2350-0999
***ScieXplore:* International Journal of Research in Science,** *10(1&2), 22-30, January-December 2023*

Experimental and Theoretical Studies on Corrosion Inhibition Performance of an Expired Drug on the Corrosion of Mild Steel in the Acid Media

S. Ananth Kumar[1], S. Rameshkumar[2*], K. Velumani[2] and S. S. Subramanian[3]

[1]Sri Venkateswara Arts and Science College, Department of Chemistry, Dharmapuri –636809, Tamil Nadu, India
[2]Sri Vasavi College, Department of Chemistry, Erode – 638316, Tamil Nadu, India; srksvc2016@gmail.com
[3]PSG College of Technology, Department of Applied Sciences, Coimbatore – 641004, Tamil Nadu, India

Abstract

Through weight loss, electrochemical impedance, and potentiodynamic polarisation techniques, the effectiveness of an expired drug in preventing the corrosion of mild steel in acidic environments was investigated. The concentration of inhibitor correlated with the corrosion inhibition efficiency, which peaked in both acid media at 100 µM. The compound is a mixed-type inhibitor of corrosion. The experimental data were connected with computed quantum chemical parameters. According to theoretical studies, the protonated form of corrosion inhibitor contributes more to the observed corrosion inhibition efficacy in acidic conditions than the neutral form.

Keywords: Corrosion, Electrochemical Impedance, Inhibitor, Potentiodynamic Polarisation

1. Introduction

The corrosion of mild steel becomes a very important topic in research due to its severe dissolution in acid media particularly in store tanks and acid refineries[1]. Most industries use acid solutions for the removal of undesired rust and scale which also leads to corrosion. Corrosion of mild steel gained considerable attention in research from the past few decades due to economic and safety consequences[2-4]. Organic compounds, in general, are found to exhibit great contribution in reducing the corrosion rate of mild steel and other iron alloys in acid media[5-7]. Such organic compounds have heteroatoms in their molecular structure and show much contribution towards reduction in corrosion rate through the heteroatoms having one or more lone pairs of electrons that are involved in the coordinate covalent bond formation with the surface iron atoms[8,9]. However, many organic compounds are not eco-friendly and cause some other environmental problems while used as corrosion inhibitors[10]. Hence, an attempt is made to use eco-friendly organic compounds as corrosion inhibitors for controlling the corrosion of mild steel in acid media. The expired drugs, the drugs which have lost their pharmaceutical activities on prolonged storage, satisfy all the requirements of a good corrosion inhibitor and could be used as corrosion inhibitors which are biodegradable and not toxic to the environment. In the present work, an attempt is made to evaluate the corrosion inhibition performance of an expired drug baclofen using weight loss, electrochemical impedance spectroscopy and potentiodynamic polarization studies. The structure and IUPAC name of the drug molecule is shown in Figure 1.

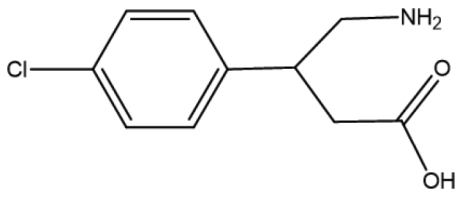

Figure 1. Structure of the drug molecule (baclofen IUPAC name-2-(4-chlorophenyl)-3-aminobutyric acid).

**Author for correspondence*

Quantum chemical studies have also been made to substantiate the experimental studies.

2. Materials and Methods

2.1 Chemicals

The expired drug is collected from a local medical shop. The chemicals used were analytical grade. The acid solutions were diluted to the required concentrations using double distilled water. The solutions of inhibitor were also prepared using double distilled water.

2.2 Mild Steel Specimens

Mild steel specimens in the form of coupons of composition C(0.22%), Si(0.38%), Mn(0.28%), S(0.044%), Cr(0.19%), Ni(0.18%), Cu(0.38%), Mo(0.018%) and rest being iron were used. The total exposed area of mild steel specimens is 0.25 cm2. The specimens were polished well using emery sheets of various grades (1/0,2/0,3/0,4/0 and 5/0) and washed with double distilled water. Then specimens were degreased with acetone. The dried specimen was weighed and immersed in the acid solutions with and without inhibitor.

2.3 Weightloss Measurements

The weighed mild specimens were immersed in the acid solutions with and without inhibitors. After three hours the mild steel specimens were taken out from the acid solutions with and without inhibitor, washed with double distilled water and degreased with acetone before weighing. From the weight, the corrosion rate is calculated using the expression;

$$Corrosion\ rate = \left(\frac{w - w'}{w}\right) \times 100$$

where w is the weight loss in the absence of corrosion inhibitor and w' is weight loss in the presence of inhibitor in acid solutions.

2.4 Electrochemical Impedance Spectroscopy

Using a three-electrode setup, the corrosion of mild steel was also investigated in the presence and absence of corrosion inhibitors at different concentrations. The working electrode was a mild steel cylindrical rod coated with Teflon, the same composition utilized in the weight loss trial, and the counter electrode was Pt foil. The reference electrode was a saturated calomel electrode. By superimposing an AC sinusoidal voltage with an amplitude of 10 mV, impedance spectra were acquired for the corrosion of mild steel in the presence and absence of corrosion inhibitors at the open circuit potential. Charge transfer resistance values are derived from the impedance investigations and used to calculate the corrosion inhibition efficiency using a formula[11,12];

$$Corrosion\ inhibition\ efficiency = \left(\frac{R'_{ct} - R_{ct}}{R_{ct}}\right) \times 100$$

where, R_{ct} and R'_{ct} are charge transfer resistance values in the absence and presence of inhibitors in the acid solutions respectively.

2.5 Potentiodynamic Polarization Method

Potentiodynamic polarization curves were recorded using the same three-electrode cell setup that was utilized to obtain impedance spectra. To record the polarization curves, a sweeping potential of 1.67 mV/s was used to transition from a more cathodic to anodic to open circuit potential by 350 mV through open circuit potential. The polarization plots were used to compute the corrosion current density, corrosion potential, and other potentiodynamic polarization parameters. The expression[11,12] was used to compute the corrosion inhibition efficiency;

$$Corrosion\ inhibition\ efficiency = \left(\frac{i_c - i'_c}{i_c}\right) \times 100$$

where, i_c and i'_c are corrosion current density values in the absence and presence of inhibitor in 1.0 M HCl and 0.5 M H_2SO_4 acid solutions respectively.

2.6 Scanning Electron Microscopy

SEM images were used to analyze the surface morphology of mild steel specimens that had corroded in solutions of 1.0 M HCl and 0.5 M H_2SO_4. The model number for the scanning electron microscope used was JEOL-JSM-6390.2.7

2.7 Quantum Chemical Calculations

The molecular properties of the molecule 2-(4-chlorophenyl)-3-aminobutyric acid were evaluated using quantum chemical studies. The geometry of the inhibitor molecule was optimized first and then the molecular properties were calculated. All the theoretical studies have been performed using density functional

theory using hybrid functional B3LYP[12-14] and the 6-31G(d,p) basis set[4,13], employing the Gaussian 98 code.

3. Results and Discussion

3.1 Weightloss Measurements

Table 1 displays the corrosion inhibition efficiency values that were determined using the weight loss measurement. This table makes it evident that the inhibitor's concentration affected the corrosion inhibition efficiency, which peaked at 100 µM concentration in both the 0.5 M H_2SO_4 acid solution and the 1.0 M HCl solution. The increased surface covering of inhibitor molecules is thought to be the cause of the increase in corrosion inhibition efficiency with inhibitor concentration. The metal surface can be effectively separated from the corroding media by the inhibitor molecules, which can cover the maximal surface area at the optimal concentration. Additionally, it is evident that in both acid media, the corrosion inhibition values are nearly identical at the ideal inhibitor concentration.

3.2 Electrochemical Impedance Spectroscopy

Figures 2 and 3 show the electrochemical impedance spectra obtained for the corrosion of mild steel in 1.0 M HCl and 0.5 M H_2SO_4 acid solutions in the presence and absence of 2-(4-chlorophenyl)-3-aminobutyric acid. The charge transfer resistance value rose as the inhibitor concentration grew, as shown by the Nyquist plots. The semicircle's increased diameter in the Nyquist plots illustrates this. It is not possible to directly derive the electrochemical impedance parameters from the Nyquist plots. To obtain the electrochemical impedance parameters, equivalent circuits are used. Figure 4 displays the Randles circuit that fits the study's needs the best[11,12]. This circuit was used to fit the experimental Nyquist plots, and the electrochemical impedance parameters were obtained. The electrochemical impedance parameters of mild steel corrosion in 1.0 M HCl and 0.5 M H_2SO_4 acid solutions at different concentrations are shown in Table 2 in both the presence and absence of 2-(4-chlorophenyl)-3-aminobutyric acid. It is evident from the table that as the inhibitor concentration grew, so did the corrosion

Table 1. The corrosion inhibition efficiency of 2-(4-chlorophenyl)-3-aminobutyric acid on corrosion of mild steel in acid media from weight loss data.

Medium	Concentration of the inhibitor (µM)	Corrosion rate (mpy)	Inhibition efficiency (I.E%)
1.0 M HCl	Blank	189	-
	1	64.3	66
	5	52.9	72
	10	49.1	74
	50	36.7	81
	100	22.7	88
0.5M H_2SO_4	Blank	286	-
	1	108	62
	5	94.4	67
	50	57.2	80
	100	40.0	86

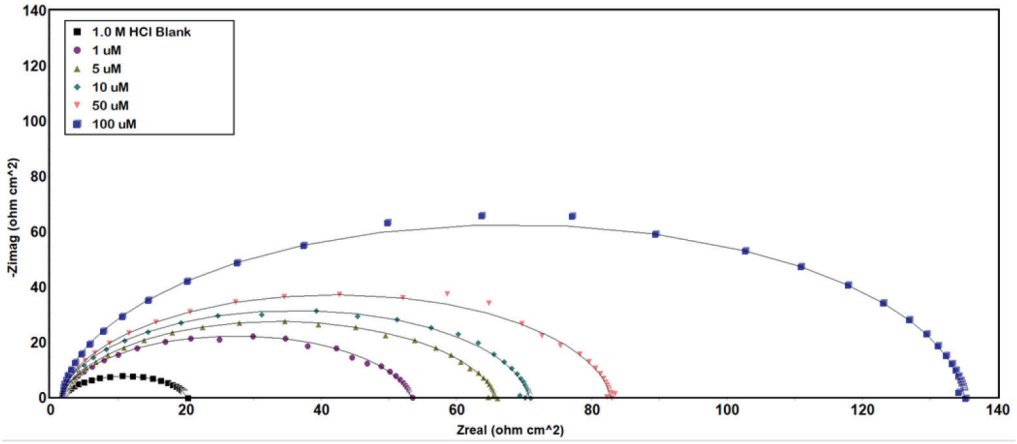

Figure 2. Nyquist plots for corrosion of mild steel in 1.0 M HCl solutions in the absence and presence of 2-(4-chlorophenyl)-3-aminobutyric acid.

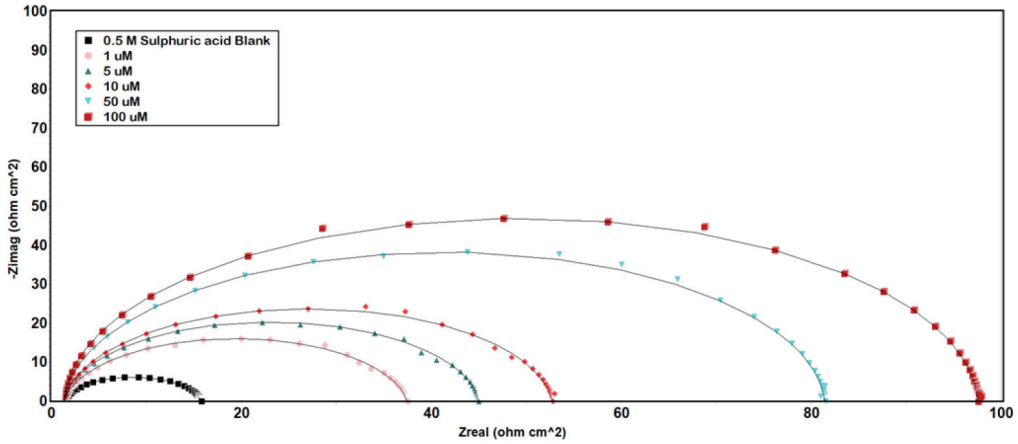

Figure 3. Nyquist plots for corrosion of mild steel in 0.5 M H_2SO_4 acid solutions in the absence and presence of 2-(4-chlorophenyl)-3-aminobutyric acid.

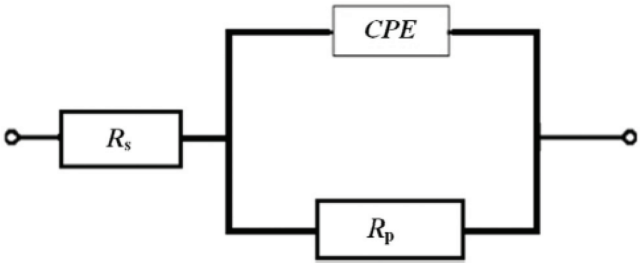

Figure 4. Equivalent circuit representing mild steel/acid solution interface.

inhibition efficiency. The charge transfer resistance value also increased as the inhibitor concentration increased, showing that the inhibitor molecules' surface covering was impeding the metal's ability to dissolve[15-17].

3.3 Potentiodynamic Polarization Studies

Figures 5 and 6 show the Tafel plots that were recorded for the mild steel corrosion in 1.0 M HCl and 0.5 M H_2SO_4 solutions. These numbers demonstrate how the presence

Table 2. Electrochemical impedance parameters derived from the Nyquist plots for the corrosion of mild steel in the absence and presence of 4-amino-3-(4-chlorophenyl) butanoic acid in 1.0 M HCl and 0.5 M H_2SO_4 solutions

Medium	Concentration of the inhibitor (µM)	(Rct)	n	Cdl(µFcm^{-2})	Inhibition Efficiency (I.E%)
1.0M HCl	Blank	18.7	0.897	407	-
	1	51.9	0.911	214	64
	5	64.5	0.905	105	71
	10	69.3	0.944	98	73
	50	81.3	0.948	73	77
	100	133.6	0.961	21	86
0.5M H_2SO_4	Blank	14.4	0.916	377	-
	1	36.0	0.927	166	60
	5	43.6	0.956	127	67
	10	51.4	0.951	82	72
	50	80.1	0.971	44	82
	100	96.2	0.981	19	85

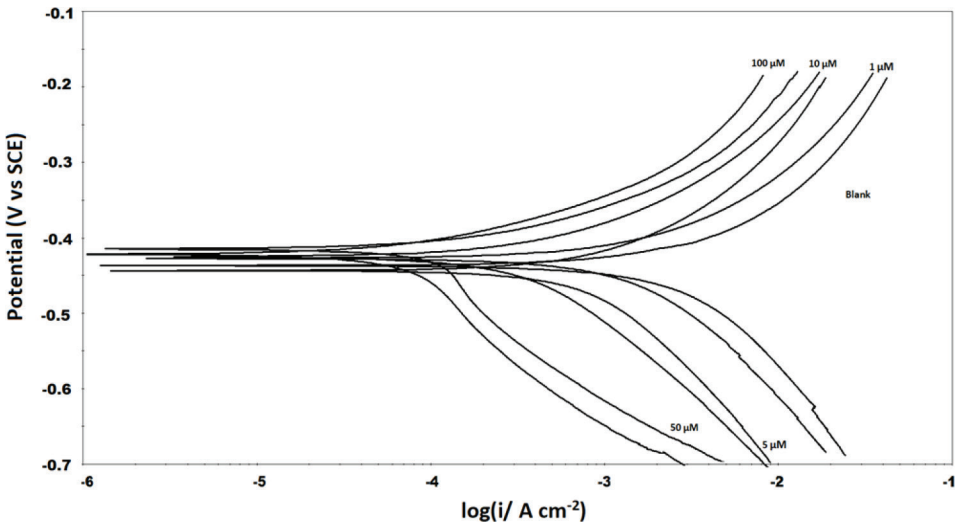

Figure 5. Tafel plots for the corrosion of mild steel in 1.0 M HCl solutions in the absence and presence of 2-(4-chlorophenyl)-3-aminobutyric acid.

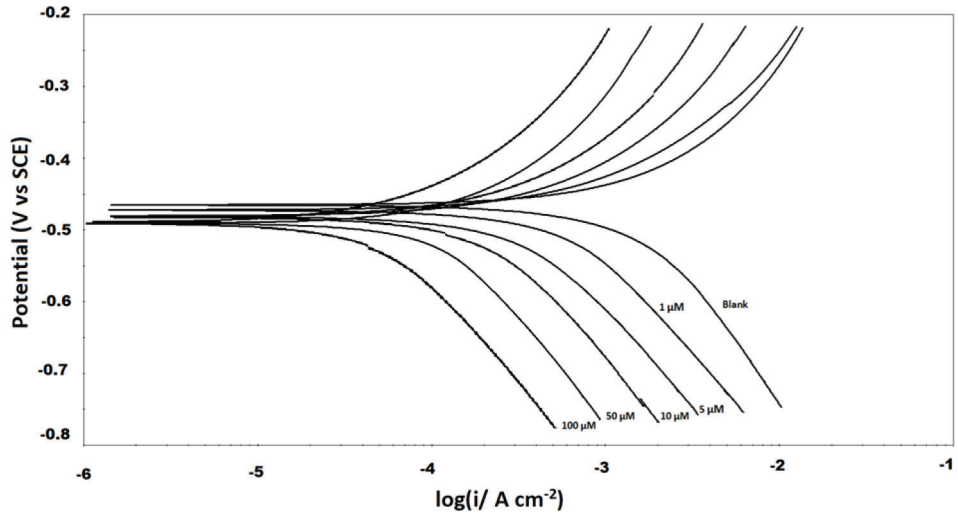

Figure 6. Tafel plots for the corrosion of mild steel in 0.5 M H_2SO_4 acid solutions in the absence and presence of 2-(4-chlorophenyl)-3-aminobutyric acid.

of an inhibitor influences mild steel corrosion in both cathodic and anodic regions. This suggests that there is a mixed type of inhibitor. Table 3 displays the possible dynamic polarization parameters that were obtained using Tafel plots. The corrosion potential of blank acid solutions does not significantly change in the presence of an inhibitor from its open circuit potential. This supports the inhibitor's mixed-type nature even further.

3.4 Scanning Electron Microscopy

The surface morphology of a mild steel specimen in 1.0 M HCl and 0.5 M H_2SO_4 acid solutions, both with and without 2-(4-chlorophenyl)-3-aminobutyric acid, is depicted in Figure 7. The SEM images demonstrate how an inhibitor efficiently increases surface morphology. This figure shows how the inclusion of an inhibitor in these two acid solutions significantly reduces the numerous cracks and localized corrosions on the mild steel surface.

3.5 Quantum Chemical Calculations

The corrosion inhibition efficiency of the drug molecule was correlated with its molecular properties through the molecular properties of the inhibitor molecules evaluated

Table 3. Potentiodynamic polarization parameters for the corrosion of mild steel in the absence and presence of 4-amino-3-(4-chlorophenyl) butanoic acid in 1.0 M HCl and 0.5 M H_2SO_4 solutions.

Medium	Concentration of the inhibitor (µM)	Corrosion Potential (Ecorr mV)	Tafel Constants		Corrosion current density ($mAcm^{-2}$)	Inhibitor efficiency (I.E%)
			βa	βc		
1.0M HCl	Blank	-445	163	217	2.784	-
	1	-409	173	209	1.031	63
	5	-427	166	198	0.835	70
	10	-434	165	212	0.779	72
	50	-409	168	227	0.612	78
	100	-417	179	215	0.389	86
0.5M H_2SO_4	Blank	-457	262	438	3.118	-
	1	-467	267	442	1.247	60
	5	-471	266	437	1.028	67
	10	-479	261	431	0.904	71
	50	-476	273	446	0.623	80
	100	-487	277	439	0.498	84

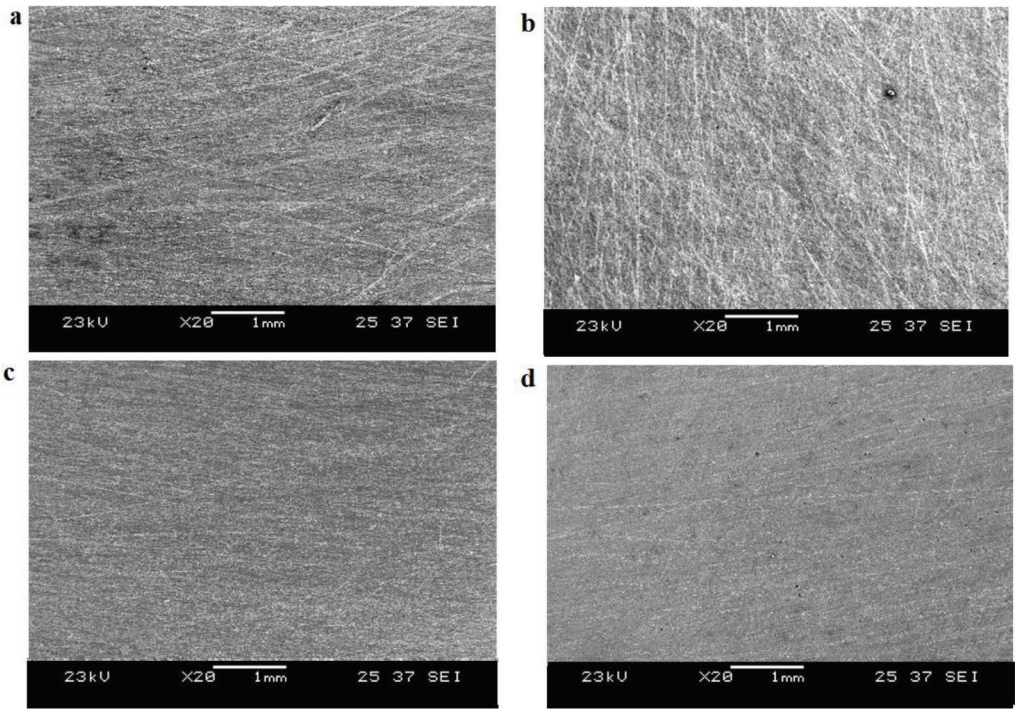

Figure 7. Sem monographs of mild steel in **a)** 1.0 M HCl **b)** 0.5 M H_2SO_4 **c)** 1.0 M HCl acid solution containing 100 µM inhibitor and **d)** 0.5 M H_2SO_4 acid solution containing 100 µM inhibitor.

using density functional theory. The geometry of the molecule was first optimized fully in the gas phase before evaluating the molecular properties. The lone pair of electrons on the nitrogen atom can also get protonated in acid solutions. Therefore, for the protonated form of the inhibitor molecule, additional quantum chemical computations as well as geometrical optimization were performed. Figure 8 shows the optimal structures of the inhibitor molecule in both its neutral and protonated versions.

Figures 9 and 10 show the distribution of electrical charges in the neutral and protonated versions of the inhibitor molecule. These graphs allow us to identify the

parts of the molecule that interact with the metal surface at very high electron densities. These graphs demonstrate how protonation significantly lowers the electron density on the hetero atom and how the electrical charge distribution resembles that of a neutral molecule's LUMO. Table 4 data displays the inhibitor molecule's neutral and protonated quantum chemical properties.

The energy of the highest occupied molecular orbital decides the tendency to donate the electrons to the surface iron atoms[12]. The protonated form has a higher energy for HOMO than the neutral form, hence the protonated form has a relatively more tendency to donate electron pairs to the metal atoms on the surface of the metal than the neutral form. The energy of the lowest unoccupied molecular orbital decides the tendency of the inhibitor to accept the electrons from the metal atoms[12]. The lower the energy of LUMO higher the tendency to accept electrons from the filled orbitals of metal atoms. In the present case,

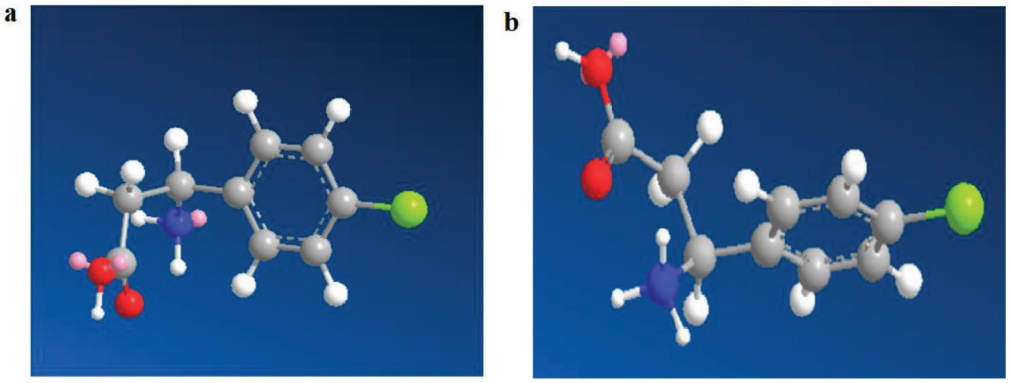

Figure 8. The optimized geometries of **a)** Neutral and **b)** Protonated forms of inhibitor molecule.

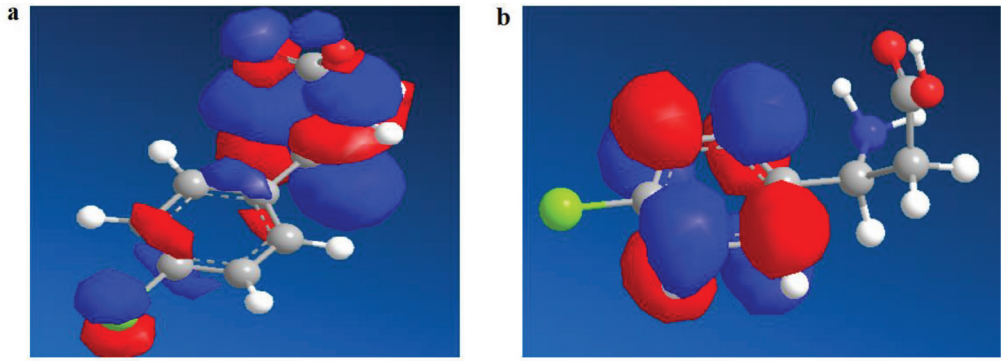

Figure 9. The electronic charge distribution in the **a)** HOMO and **b)** LUMO of neutral form of inhibitor molecule.

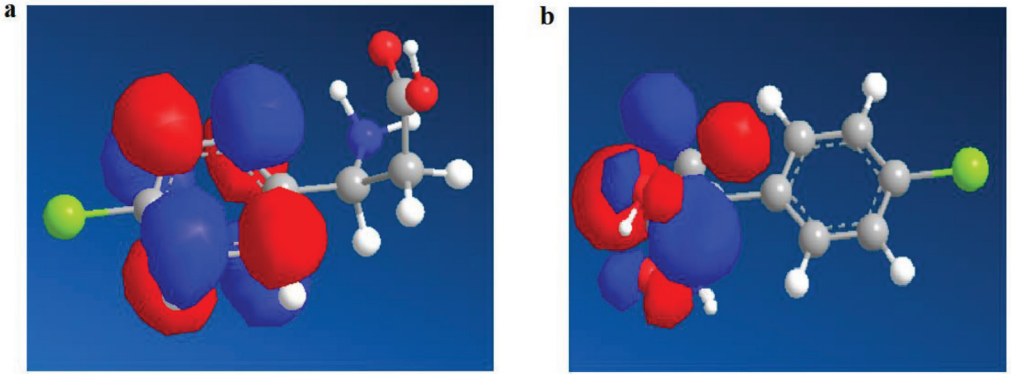

Figure 10. The electronic charge distribution in the **a)** HOMO and **b)** LUMO of protonated inhibitor molecule.

Table 4. Quantum chemical parameters calculated for the neutral and protonated forms of the inhibitor molecule

S. No.	Quantum chemical parameters	Neutral molecule	Protonated form
1	Total energy (eV)	-2284.58666	-2297.68037
2	ELUMO (eV)	-0.446	-0.183
3	EHOMO (eV)	-9.708	-8.699
4	ΔE (eV)	-9.262	-8.516
5	Ionization potential (I/eV)	0.446	0.183
6	Electron affinity (A/eV)	9.708	8.699
7	Hardness (η/ev)	-4.631	-4.258
8	Softness (S/eV)	-0.107968041	-0.117426022
9	Electronegativity (χ)	5.077	4.441
10	Electrophilicity (ω)	-2.782976571	-2.31593248
11	Fraction of electrons transferred (Δ N)	-0.207622544	-0.300493189
12	Dipole moment	3.12548	3.64309

the neutral form of the inhibitor molecule has a relatively lower value for the energy of LUMO than the protonated form[12]. Hence, the back donation is much more favourable in the neutral form of the inhibitor molecule. The lower the ionization energy higher the tendency to donate electrons for bond formation and hence higher the corrosion inhibition[12, 18-21]. In the present case again the protonated form has a relatively lower ionization energy than the neutral form and hence it must show a relatively higher contribution to the corrosion inhibition efficiency[12]. Similarly, the inhibitor molecule with lower electron affinity has more tendency to donate electrons for the bond formation. The protonated form with a lower electron affinity than the neutral form may have more electron donating tendency than the neutral form. In general, all the quantum chemical parameters calculated suggest that the protonated form must show a relatively higher contribution to the observed corrosion inhibition than the neutral form of the inhibitor molecule.

4. Conclusion

The following are important conclusions arrived at in the present study.

i. The drug molecule that has expired may still be useful as a corrosion inhibitor in solutions of HCl and H_2SO_4.
ii. The inhibitor's efficacy in inhibiting corrosion rose as concentration did, peaking at an ideal inhibitor concentration of 100 μM.
iii. The weightloss and electrochemical impedance studies suggested that a protective film is formed on the metal surface in acid media to reduce corrosion.
iv. The potentiodynamic polarization studies implied that the inhibitor is of mixed type.
v. Quantum chemical calculations suggested that the protonated form of the inhibitor molecule has a relatively higher contribution to the observed corrosion inhibition efficiency than the neutral form.

5. References

1. Varshney K, Varshney PK, Gautam K, Tanwar M, Chaudhary M. Current trends and future perspectives in the recycling of spent lead acid batteries in India. Materials Today: Proceedings. 2020; 26:592-602. https://doi.org/10.1016/j.matpr.2019.12.168
2. Teng JG, Yu T, Fernando D. Strengthening of steel structures with fiber-reinforced polymer composites. Journal of Constructional Steel Research. 2012; 78:131-43. https://doi.org/10.1016/j.jcsr.2012.06.011
3. Ates M. A review on conducting polymer coatings for corrosion protection. Journal of Adhesion Science and Technology. 2016; 30(14):1510-36. https://doi.org/10.1080/01694243.2016.1150662
4. Angst UM. Challenges and opportunities in corrosion of steel in concrete. Materials and Structures. 2018; 51(1):1-20. https://doi.org/10.1617/s11527-017-1131-6
5. Bahrami MJ, Hosseini SM, Pilvar P. Experimental and theoretical investigation of organic compounds as inhibitors for mild steel corrosion in sulfuric acid medium. Corrosion science. 2010; 52(9):2793-803. https://doi.org/10.1016/j.corsci.2010.04.024

6. Schmitt G. Application of inhibitors for acid media: report prepared for the European federation of corrosion working party on inhibitors. British Corrosion Journal. 1984; 19(4):165-76. https://doi.org/10.1179/000705984798273100
7. Khadom AA, Abd AN, Ahmed NA. Xanthium strumarium leaves extracts as a friendly corrosion inhibitor of low carbon steel in hydrochloric acid: Kinetics and mathematical studies. South African Journal of Chemical Engineering. 2018; 25:13-21. https://doi.org/10.1016/j.sajce.2017.11.002
8. Lgaz H, Lee HS. The effect of heterocyclization of 2-mercaptobenzimidazole on its strength of coordination to iron: A dispersion-corrected DFT study. Applied Surface Science. 2021; 567. https://doi.org/10.1016/j.apsusc.2021.150819
9. Rani BE, Basu BB. Green inhibitors for corrosion protection of metals and alloys: An overview. International Journal of corrosion. 2012; 2012. https://doi.org/10.1155/2012/380217
10. Zaferani SH, Sharifi M, Zaarei D, Shishesaz MR. Application of eco-friendly products as corrosion inhibitors for metals in acid pickling processes - A review. Journal of Environmental Chemical Engineering. 2013; 1(4):652-7. https://doi.org/10.1016/j.jece.2013.09.019
11. Mallaiya K, Subramaniam R, Srikandan SS, Gowri S, Rajasekaran N, Selvaraj A. Electrochemical characterization of the protective film formed by the unsymmetrical Schiff's base on the mild steel surface in acid media. Electrochimica Acta. 2011; 56(11):3857-63. https://doi.org/10.1016/j.electacta.2011.02.036
12. Kumar SR, Danaee I, Avei MR, Vijayan M. Quantum chemical and experimental investigations on equipotent effects of (+) R and (−) S enantiomers of racemic amisulpride as eco-friendly corrosion inhibitors for mild steel in acidic solution. Journal of Molecular Liquids. 2015; 212:168-86. https://doi.org/10.1016/j.molliq.2015.09.001
13. Machado SF, Camiletti GG, Neto AC, Jorge FE, Jorge RS. Gaussian basis set of triple zeta valence quality for the atoms from K to Kr: Application in DFT and CCSD (T) calculations of molecular properties. Molecular Physics. 2009; 107(16):1713-27. https://doi.org/10.1080/00268970903042258
14. Yang S, Olishevski P, Kertesz M. Bandgap calculations for conjugated polymers. Synthetic Metals. 2004; 141(1-2):171-7. https://doi.org/10.1016/j.synthmet.2003.08.019
15. Chauhan LR, Gunasekaran G. Corrosion inhibition of mild steel by plant extract in dilute HCl medium. Corrosion Science. 2007; 49(3):1143-61. https://doi.org/10.1016/j.corsci.2006.08.012
16. Satpati AK, Ravindran PV. Electrochemical study of the inhibition of corrosion of stainless steel by 1, 2, 3-benzotriazole in acidic media. Materials Chemistry and Physics. 2008; 109(2-3):352-9. https://doi.org/10.1016/j.matchemphys.2007.12.002
17. Singh A, Lin Y, Obot IB, Ebenso EE, Ansari KR, Quraishi MA. Corrosion mitigation of J55 steel in 3.5% NaCl solution by a macrocyclic inhibitor. Applied Surface Science. 2015; 356:341-7. https://doi.org/10.1016/j.apsusc.2015.08.094
18. Sulaiman KO, Onawole AT. Quantum chemical evaluation of the corrosion inhibition of novel aromatic hydrazide derivatives on mild steel in hydrochloric acid. Computational and Theoretical Chemistry. 2016; 1093:73-80. https://doi.org/10.1016/j.comptc.2016.08.014
19. Karzazi Y, Belghiti ME, Dafali A, Hammouti B. A theoretical investigation on the corrosion inhibition of mild steel by piperidine derivatives in hydrochloric acid solution. Journal of Chemical and Pharmaceutical Research. 2014; 6:689-96.
20. Upadhyay A, Purohit AK, Mahakur G, Dash S, Kar PK. Verification of corrosion inhibition of Mild steel by some 4-Aminoantipyrine-based Schiff bases-Impact of adsorbate substituent and cross-conjugation. Journal of Molecular Liquids. 2021;333. https://doi.org/10.1016/j.molliq.2021.115960
21. Zhang F, Tang Y, Cao Z, Jing W, Wu Z, Chen Y. Performance and theoretical study on corrosion inhibition of 2-(4-pyridyl)-benzimidazole for mild steel in hydrochloric acid. Corrosion Science. 2012; 61:1-9. https://doi.org/10.1016/j.corsci.2012.03.045